Global Scaling of Planetary Atmospheres

Hartmut Müller
E-mail: hm@interscalar.com

We derive a model of the stratification of planetary atmospheres as application of our scale-invariant model of matter as fractal chain system of oscillating protons and electrons. Model claims are verified by aerological, geophysical and planetological data.

Introduction

The vertical stratification of the Earth's atmosphere is caused by very different processes and it is a complex field of research. In general, air pressure and density decrease exponentially with altitude, but temperature, ionization and chemical composition have more complicated profiles. The standard division into troposphere, stratosphere, mesosphere, thermosphere, ionosphere and exosphere is based on satellite, airplane and ground measurements and considers aerodynamic, hydrodynamic, thermodynamic, chemical, electromagnetic, gravitational factors in their complex interaction.

New measurements of the atmospheres of solar system planets and moons over the past four decades from various spacecraft missions have been used to characterize the structure and dynamics of these atmospheric environments and to compare them to one another. A corresponding evolution of modeling tools occurs, from simple to complex frameworks.

Terrestrial modeling frameworks like HAMMONIA [1], ECHAM [2], IRI [3] and CMAM [4] of numerical modeling have been used to launch simulations [5] of other planetary upper atmospheres and ionospheres. The primary benefit of the Earth paradigm can be realized for other planetary upper atmospheres having similarities in their fundamental planetary parameters, basic processes and vertical domains (atmospheric layers).

In fact, stratification as atmospheric feature is associated not only with Earth, but occurs on any other planet or moon that has an atmosphere as well. Furthermore, stable atmospheric boundaries like tropopause, stratopause, thermopause and mesopause have similar vertical distributions at different celestial bodies in atmospheres of very different chemical compositions.

In this paper we apply our scale-invariant model [6] of matter as fractal chain system of oscillating protons and electrons and develop a general model of planetary atmospheric stratification that might help to understand the processes sustaining the observed stable atmospheric structures.

Methods

In [7] we have shown that the set of natural frequencies of a fractal chain system of similar harmonic oscillators can be described as set of finite continued fractions $\mathcal{F}$ (1), which are natural logarithms, where ω_{jk} is the set of angular frequencies and ω_{00} is the fundamental frequency of the set. The denominators are integer: $n_{j0}, n_{j1}, n_{j2}, \ldots, n_{jk} \in \mathrm{Z}$, the cardinality $j \in \mathrm{N}$ of the set and the number $k \in \mathrm{N}$ of layers are finite:

$$\ln(\omega_{jk}/\omega_{00}) = n_{j0} + \cfrac{z}{n_{j1} + \cfrac{z}{n_{j2} + \ddots + \cfrac{z}{n_{jk}}}} = [z, n_{j0}; n_{j1}, n_{j2}, \ldots, n_{jk}] = \mathcal{F}. \quad (1)$$

In the canonical form, the numerator z equals 1 and for finite continued fractions the distribution density of the eigenvalues reaches maxima near reciprocal integers 1, 1/2, 1/3, 1/4, ... which are the attractor points of the fractal set $\mathcal{F}$ of natural logarithms (fig. 1).

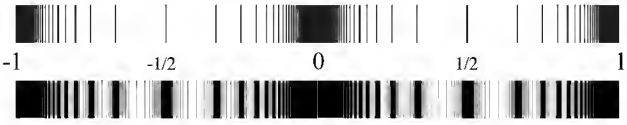

Fig. 1: The canonical form of $\mathcal{F}$ for $k = 1$ (above) and for $k = 2$ (below) in the range $-1 \leqslant \mathcal{F} \leqslant 1$.

Any finite continued fraction represents a rational number [8]. Therefore, all natural frequencies ω_{jk} in (1) are irrational, because for rational exponents the natural exponential function is transcendental [9]. This circumstance provides for high stability of eigenstates in a fractal chain system of harmonic oscillators because it prevents resonance interaction between the elements of the system [10]. Already in 1987 we have applied continued fractions of the type $\mathcal{F}$ as criterion of stability in engineering [11, 12].

In the case of harmonic quantum oscillators, the continued fractions $\mathcal{F}$ define not only fractal sets of natural angular frequencies ω_{jk}, angular accelerations $a_{jk} = c \cdot \omega_{jk}$, oscillation periods $\tau_{jk} = 1/\omega_{jk}$ and wavelengths $\lambda_{jk} = c/\omega_{jk}$ of the chain system, but also fractal sets of energies $\mathrm{E}_{jk} = \hbar \cdot \omega_{jk}$ and masses $\mathrm{m}_{jk} = \mathrm{E}_{jk}/c^2$ which correspond with the eigenstates of the system. For this reason, we call the continued fraction $\mathcal{F}$ the "fundamental fractal" of eigenstates in chain systems of harmonic quantum oscillators.

In the canonical form ($z = 1$) of the fundamental fractal $\mathcal{F}$, shorter continued fractions correspond with more stable eigenstates of a chain system of harmonic oscillators. Therefore, integer logarithms represent the most stable eigenstates (main attractor nodes).

Property	Electron	Proton
rest mass m	$9.10938356(11) \cdot 10^{-31}$ kg	$1.672621898(21) \cdot 10^{-27}$ kg
energy $E = mc^2$	0.5109989461(31) MeV	938.2720813(58) MeV
angular frequency $\omega = E/\hbar$	$7.76344071 \cdot 10^{20}$ Hz	$1.42548624 \cdot 10^{24}$ Hz
angular oscillation period $\tau = 1/\omega$	$1.28808867 \cdot 10^{-21}$ s	$7.01515 \cdot 10^{-25}$ s
angular wavelength $\lambda = c/\omega$	$3.8615926764(18) \cdot 10^{-13}$ m	$2.1030891 \cdot 10^{-16}$ m

Table 1: The basic set of physical properties of the electron and proton. Data taken from Particle Data Group [13]. Frequencies, oscillation periods and the proton wavelength are calculated.

As the cardinality and number of layers of the continued fractions $\mathcal{F}$ are finite but not limited, in each point of the space-time occupied by the chain system of harmonic quantum oscillators the scalar $\mathcal{F}$ is defined. Therefore, any chain system of harmonic quantum oscillators can be seen as source of the scalar field $\mathcal{F}$, the fundamental field of the system.

Normal matter is formed by nucleons and electrons because they are exceptionally stable quantum oscillators. In the concept of isospin, proton and neutron are viewed as two states of the same quantum oscillator. Furthermore, they have similar rest masses. However, a free neutron decays into a proton, an electron and antineutrino within 15 minutes while the life-spans of the proton and electron top everything that is measurable, exceeding 10^{29} years [13].

The exceptional stability of electron and proton predestinate their physical characteristics as fundamental units. Table 1 shows the basic set of electron and proton units that can be considered as a fundamental metrology (c is the speed of light in a vacuum, $\hbar$ is the Planck constant, k_B is the Boltzmann constant). In [14] was shown that the fundamental metrology (tab. 1) is compatible with Planck units [15].

We hypothesize that scale invariance of the fundamental field $\mathcal{F}$ calibrated on the physical properties of the proton and electron (tab. 1) is a universal characteristic of organized matter and criterion of stability. This hypothesis we have called 'global scaling' [16, 17].

Results

Within our scale-invariant model of matter [18], atoms and molecules emerge as eigenstates of stability in fractal chain systems of harmonically oscillating protons and electrons.

Andreas Ries [19] demonstrated that this model allows for the prediction of the most abundant isotope of a given chemical element. From this point of view, any physical body, being solid, liquid or gas can be seen as fractal chain system of oscillating molecules, atoms, ions, protons and electrons that generates its fundamental field $\mathcal{F}$.

Therefore, in the framework of our fractal model of matter, the fundamental field $\mathcal{F}$ affects any type of physical interaction, including the gravitational. In [20] we applied our model to the analysis of gravimetric and seismic characteristics of the Earth and could show [21] that our estimations correspond well with established empiric models of the Earth interior.

In this paper we demonstrate that the vertical sequence of stable atmospheric layers corresponds with the sequence of main equipotential surfaces of the fundamental field $\mathcal{F}$, not only at Earth, but also at Venus, Mars and Titan. Table 2 gives an overview of this correspondence.

The lowest layer of Earth's atmosphere is the troposphere where nearly all weather conditions take place. The average height of the troposphere is 20 km in the tropics, 12 km in the mid latitudes, and 7 km in the polar regions in winter [22]. Table 2 and fig. 2 show the correspondence of these tropospheric levels with the main equipotential surfaces [37; 2] = 7.5 km, [38; ∞] = 12 km and [38; 2] = 20 km of the fundamental field $\mathcal{F}$, calibrated on the electron wavelength.

At its lowest part, the planetary boundary layer (PBL), the troposphere displays turbulence and strong vertical mixing due to the contact with the planetary surface. The top of the PBL in convective conditions is often well defined by the existence of a stable capping inversion, into which turbulent motions from beneath are generally unable to penetrate [23]. The height of this elevated stable layer is quite variable, but is generally below 3 km. Over deserts in mid-summer under strong surface heating the PBL may rise to 4 - 5 km. In the temperate zones, it can be defined by the quite sharp decrease of aerosol concentration at the height of about 1600 m. Over the open oceans, but also at night over land, under clear skies and light winds, with a capping stratocumulus, the depth of the PBL may be no more than 600 m.

Table 2 and fig. 2 show the correspondence of the PBL features with the main equipotential surfaces [35; ∞] = 600 m, [36; ∞] = 1600 m and [37; ∞] = 4.5 km of the fundamental field $\mathcal{F}$, calibrated on the electron wavelength. It is noticeable that in 1992 Hess [24] already reviewed scaling aspects of the boundary layer.

Above the PBL, where the wind is nearly geostrophic, vertical mixing is less and the free atmosphere density stratification initiates. The jet stream flows near the boundary

BOUNDARY OF ATMOSPHERIC LAYER	ALTITUDE h, KM	$\ln(h/\lambda_e)$	$\mathcal{F}$
van Allen outer electron belt max density	13000	44.96	[45; ∞]
	8200		[44; 2]
	5000		[44; ∞]
van Allen inner proton belt max density	3000	43.50	[43; 2]
Earth exopause	1800	42.99	[43; ∞]
	1100		[42; 2]
Earth thermopause	650	41.97	[42; ∞]
	400		[41; 2]
Venus & Mars thermopause, Venus atmospheric entry	250	41.01	[41; ∞]
Earth atmospheric entry, Venus mesopause	150	40.50	[40; 2]
Earth & Titan mesopause, Venus tropopause, Mars stratopause & entry	90	39.99	[40; ∞]
Earth & Titan stratopause	55	39.50	[39; 2]
Titan tropopause	33	38.99	[39; ∞]
Earth tropic tropopause	20	38.49	[38; 2]
Earth temperate tropopause	12	37.98	[38; ∞]
Earth polar tropopause	7.5	37.51	[37; 2]
desert summer PBL inversion	4.5	37.00	[37; ∞]
continental PBL inversion	1.6	35.96	[36; ∞]
marine PBL inversion	0.6	34.98	[35; ∞]

Table 2: Altitudes of the boundaries of various atmospheric layers on Earth, Venus, Mars and Titan and their correspondence with main equipotential surfaces of the fundamental field $\mathcal{F}$, calibrated on the electron wavelength.

between the troposphere and the stratosphere. As altitude increases, the temperature of the troposphere generally decreases until the tropopause.

At the bottom of the stratosphere, above the tropopause, the temperature doesn't change much, but at the inverse layer at altitudes between 20 and 33 km the temperature increases from -50°C to 0°C. Then at the stratopause at 55 km altitude the temperature stabilizes. It is the boundary between two layers: the stratosphere and the mesosphere [25]. The ozone layer (ozonosphere) of the stratosphere absorbs most of the Sun's ultraviolet radiation and is mainly found at altitudes between 12 and 30 km, with the highest intensity of formation at 20 km height [26].

Table 2 and fig. 2 show the correspondence of the main stratosphere layers with the main equipotential surfaces [39; ∞] = 33 km and [39; 2] = 55 km of the fundamental field $\mathcal{F}$, calibrated on the electron wavelength.

Above the stratopause, in the mesosphere between 55 and 90 km altitude [27], the temperature decreases again, reaching about -100 °C at the mesopause [28]. This altitude coincides with the turbopause: above this level the atmosphere is of extremely low density so that the chemical composition is not mixed but stratified and depends on the molecular masses. Table 2 and fig. 2 show the correspondence of the mesopause with the main equipotential surface [40; ∞] = 90 km of the fundamental field $\mathcal{F}$, calibrated on the electron wavelength.

Above the mesopause, in the thermosphere, the (kinetic) temperature increases and can rise to 1000 °C (depending on solar activity) at altitudes of 250 km remaining quasi stable with increasing height. Due to solar radiation, gas molecules dissociate into atoms: above 90 km dissociate carbon dioxygen and dihydrogen, above 150 km dissociates dioxygen and above 250 km dissociates dinitrogen. Above 150 km, the density is so low that molecular interactions are too infrequent to permit the transmission of sound. Table 2 and fig. 2 show the correspondence of these thermosphere layers with the main equipotential surfaces [40; 2] = 150 km and [41; ∞] = 250 km of the fundamental field $\mathcal{F}$, calibrated on the electron.

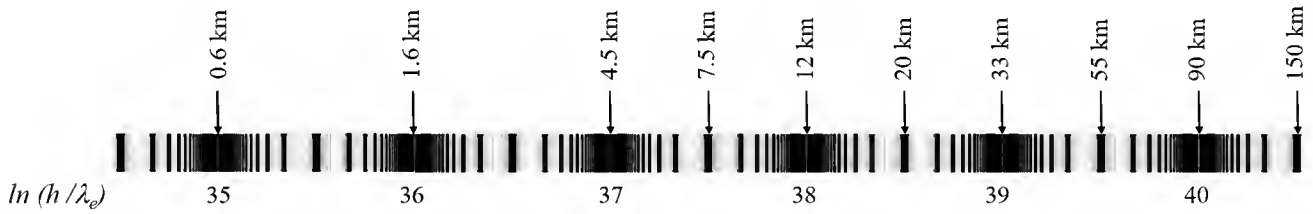

Fig. 2: The fundamental field $\mathcal{F}$ (natural logarithmic presentation) calibrated on the electron wavelength in the range $35 \leq \mathcal{F} \leq 40$ and the corresponding altitudes h in km.

The Karman line [29] is considered by the Federation Aeronautique Internationale (FAI) [30] as the border between the atmosphere and outer space, as altitude where the atmosphere becomes too thin to support aeronautical flight, since a vehicle at this altitude would have to travel faster than orbital velocity to derive sufficient aerodynamic lift to support itself. On Earth, atmospheric effects become noticeable during atmospheric entry of spacecraft already at an altitude of around 120 - 150 km, while on Venus atmospheric entry occurs at 250 km and on Mars at about 80 - 90 km above the surface. These heights mark also the bases of the anacoustic zones.

The location of the thermopause is near altitudes of 600 – 700 km and depends on solar activity [31]. Above starts the exosphere, where the atmosphere (mostly consisting of hydrogen atoms) thins out and merges with interplanetary space. This uppermost layer, until 13000 km observable from space as the geocorona, extends up to 100000 km. Table 2 and fig. 2 show the correspondence of the thermopause with the main equipotential surface [42; ∞] = 650 km of the fundamental field $\mathcal{F}$, calibrated on the electron wavelength.

The van Allen radiation belts [32] are features of Earth's magnetosphere. The inner belt consists of high energetic protons which reach their maximum concentration at altitudes of 3000 km. The outer belt consists of high energetic electrons with maximum concentration at altitudes of 13000 km.

While the outer belt maximum corresponds with the main equipotential surface [45; ∞] = 13000 km of the fundamental field $\mathcal{F}$, calibrated on the electron wavelength, the inner belt maximum corresponds with the equipotential surface [43; 2] = 3000 km that is the main equipotential surface [51; ∞] of the fundamental field $\mathcal{F}$, calibrated on the proton wavelength. In fact, the natural logarithm of the electron-to-proton wavelength ratio is approximately 7.5 and consequently, $\mathcal{F}$ calibrated on the proton will be shifted by 7.5 logarithmic units relative to the $\mathcal{F}$ calibrated on the electron:

$$\ln\left(\frac{\lambda_{\text{electron}}}{\lambda_{\text{proton}}}\right) = \ln\left(\frac{3.8615926764 \cdot 10^{-13}\ \text{m}}{2.1030891 \cdot 10^{-16}\ \text{m}}\right) \approx 7.5.$$

This circumstance, probably, can explain the high proton concentration at the inner belt.

Conclusion

The correspondence of the atmospheric stratification on the Earth, Venus, Mars and Titan with main equipotential surfaces of $\mathcal{F}$ demonstrates that the fundamental field affects very different types of physical interaction and is a strong confirmation of global scaling and our model of matter as fractal chain system of oscillating protons and electrons.

Probably, in future our model can be applied for estimation of the atmospheric stratification at ice giants like Uranus and Neptune and gas giants like Jupiter, Saturn and extrasolar planets as well.

Acknowledgements

I'm thankful to Leili Khosravi and Oleg Kalinin for valuable discussions.

Submitted on February 21, 2018

References

1. Schmidt H., Brasseur G. P. The response of the middle atmosphere to solar cycle forcing in the Hamburg Model of the neutral and ionized atmosphere. Space Science Reviews, 1–12, 2006.
2. Roeckner E. et al. Report No. 349. The atmospheric general circulation model ECHAM5. Max Planck Institute for Meteorology, Hamburg, 2003.
3. Bilitza D. et al. The International Reference Ionosphere 2012 – a model of international collaboration. Journal of Space Weather and Space Climat, 4, A07, 2014.
4. Grandpre J. de, Beagley S. R. et al. Ozone climatology using interactive chemistry: Results from the Canadian Middle Atmosphere Model. Journal of Geophysical Research, Vol. 105, No. D21, 475–491, 2000.
5. Bougher S. W. et al. Neutral Upper Atmosphere and Ionosphere Modeling. Space Science Reviews, 139: 107–141, 2008.
6. Müller H. Fractal Scaling Models of Natural Oscillations in Chain Systems and the Mass Distribution of Particles. *Progress in Physics*, vol. 3, 61–66, 2010.
7. Müller H. Fractal Scaling Models of Resonant Oscillations in Chain Systems of Harmonic Oscillators. *Progress in Physics*, vol. 2, 72–76, 2009.
8. Khintchine A.Ya. Continued fractions. University of Chicago Press, Chicago, 1964.
9. Hilbert D. Über die Transcendenz der Zahlen e und π. *Mathematische Annalen* 43, 216–219, 1893.
10. Panchelyuga V. A., Panchelyuga M. S. Resonance and Fractals on the Real Numbers Set. *Progress in Physics*, vol. 4, 48–53, 2012.

11. Müller H. The general theory of stability and objective evolutionary trends of technology. Applications of developmental and construction laws of technology in CAD. Volgograd, VPI, 1987 (in Russian).
12. Müller H. Superstability as a developmental law of technology. Technology laws and their Applications. Volgograd-Sofia, 1989 (in Russian).
13. Olive K.A. et al. (Particle Data Group), *Chin. Phys. C*, 38, 090001, 2016.
Patrignani C. et al. (Particle Data Group), *Chin. Phys. C*, 40, 100001, 2016.
14. Müller H. Scale-Invariant Models of Natural Oscillations in Chain Systems and their Cosmological Significance. *Progress in Physics*, vol. 4, 187–197, 2017.
15. Max Planck. Über Irreversible Strahlungsvorgänge. In: Sitzungsbericht der Königlich Preußischen Akademie der Wissenschaften. 1899, vol. 1, 479–480.
16. Müller H. Scaling as Fundamental Property of Natural Oscillations and the Fractal Structure of Space-Time. Foundations of Physics and Geometry. Peoples Friendship University of Russia, 2008 (in Russian).
17. Müller H. Scaling of body masses and orbital periods in the Solar System as consequence of gravity interaction elasticity. Abstracts of the XII. International Conference on Gravitation, Astrophysics and Cosmology, dedicated to the centenary of Einstein's General Relativity theory. Moscow, PFUR, 2015.
18. Müller H. Emergence of Particle Masses in Fractal Scaling Models of Matter. *Progress in Physics*, vol. 4, 44–47, 2012.
19. Ries A. Qualitative Prediction of Isotope Abundances with the Bipolar Model of Oscillations in a Chain System. *Progress in Physics*, vol. 11, 183–186, 2015.
20. Müller H. Gravity as Attractor Effect of Stability Nodes in Chain Systems of Harmonic Quantum Oscillators. *Progress in Physics*, vol. 1, 19–23, 2018.
21. Müller H. Quantum Gravity Aspects of Global Scaling and the Seismic Profile of the Earth. *Progress in Physics*, vol. 1, 41–45, 2018.
22. Danielson, Levin, and Abrams, Meteorology, McGraw Hill, 2003.
23. Garratt J. R. Review: the atmospheric boundary layer. Earth-Science Review, 37, pp. 89–134, 1994.
24. Hess G. D. Observations and scaling of the atmospheric boundary layer. Australian Meteorological Magazine. 41, 79–99 (1992).
25. Brasseur G. P., Solomon S. Aeronomy of the Middle Atmosphere. Chemistry and Physics of the Stratosphere and Mesosphere. ISBN-10 1-4020-3824-0, Springer, 2005.
26. Stolarski R. et al. Measured Trends in Stratospheric Ozone. Science, New Series, Vol. 256, Issue 5055, 342–349, 1992.
27. Holton J. R. The Dynamic Meteorology of the Stratosphere and Mesosphere. ISBN 978-1-935704-31-7, 1975.
28. Beig G., Keckhut P. Lowe R. P. et al. Review of mesospheric temperature trends. Rev. Geophys. 41 (4), 1015, 2003.
29. Karman T., Edson L. The Wind and Beyond. Little, Brown, Boston, 1967.
30. Cordoba S. F. The 100 km Boundary for Astronautics. Federation Aeronautique Internationale, 2011.
31. Beig G., Scheer J., Mlynczak M. G., Keckhut P. Overview of the temperature response in the mesosphere and lower thermosphere to solar activity. Reviews of Geophysics, 46, RG3002, July 2008.
32. Schaefer H. J. Radiation Dosage in Flight through the Van Allen Belt. Aerospace Medicine, Vol. 30, No. 9, 1959.